

## Galaxies at High Redshifts

A. Yahil, K. M. Lanzetta

*Department of Physics and Astronomy, State University of New York,  
Stony Brook, NY 11794-3800, USA*

A. Fernández-Soto

*Department of Astrophysics and Optics, School of Physics, University of New South  
Wales, Kensington-Sidney, NSW 2052, Australia*

Several conclusions have been reached over the last few years concerning high-redshift galaxies: (1) The excess of faint blue galaxies is due to dwarf galaxies. (2) Star formation peaks at redshifts  $z \approx 1 - 2$ . (3) It appears to occur piecemeal in any given galaxy and there is no evidence for starbursting throughout a large  $\sim 10$  kpc galaxy. (4) There is significant and sharp diminution in the number of  $L_*$  spiral galaxies at redshifts  $1 < z < 2$  and elliptical galaxies at redshifts  $2.5 < z < 4$ . (5) It is increasingly more difficult to “hide” large high-redshift galaxies in universes with larger volumes per unit redshift, i.e., open or  $\lambda$  models, which have lower deceleration parameters.

### 1 Introduction

This paper reviews high redshift galaxies as we understand them. It is not meant to be comprehensive. Instead, we ask the questions that seem most important to us. Why do we observe high redshift galaxies, §2? How do we observe them, §3? What have we learned from the observations, §4? And how should we continue our research, §5?

### 2 Why Observe High Redshift Galaxies?

In the standard paradigm of galaxy formation, galaxies are imagined to have formed in essentially their present shapes at some definite epoch in the past, at redshifts  $z \sim 5$ . Their stellar content is then supposed to evolve passively with time, governed only by the rate of star formation and stellar evolution. Elliptical galaxies are supposed to have a short initial star-formation phase  $\sim 1$  Gyr, while spirals and irregulars have star formation lasting 10 Gyr or longer.

The original motivation for passive-evolution was the observation of increased counts of blue galaxies at magnitudes  $B \gtrsim 24$ , which were thought to be high-redshift elliptical galaxies in their original burst of star formation.<sup>1</sup>

Today we are able directly to observe high-redshift galaxies and hence see the formation and evolution of both elliptical and spiral galaxies in action; evolution can be tested directly. Although less discussed, observations have

now been carried out sufficiently deeply to have a chance to observe the initial burst of star formation even in individual globular clusters. More generally, objects whose luminosities are well below  $L_*$  are now routinely observed at high redshift.

With systematic deep surveys it has also become possible to estimate the total rest-frame UV radiation per unit volume emitted at high redshift and to deduce the global rate of star formation.<sup>2</sup> These observations can then be compared with simulations of galaxy formation.<sup>3</sup>

Finally, the counts of galaxies as a function of redshift, luminosity, and, as we argue below, size, can be used to constrain the deceleration parameter,  $q_0$ . This is a difficult task, due to uncertainties in galaxy formation and evolution and in the dust content of young galaxies. At redshifts  $z \gtrsim 1$ , though, the difficulty is mitigated by the order-of-magnitude sensitivity of the differential comoving volume,  $dV/dz$ , to the deceleration parameter, Fig. 1.

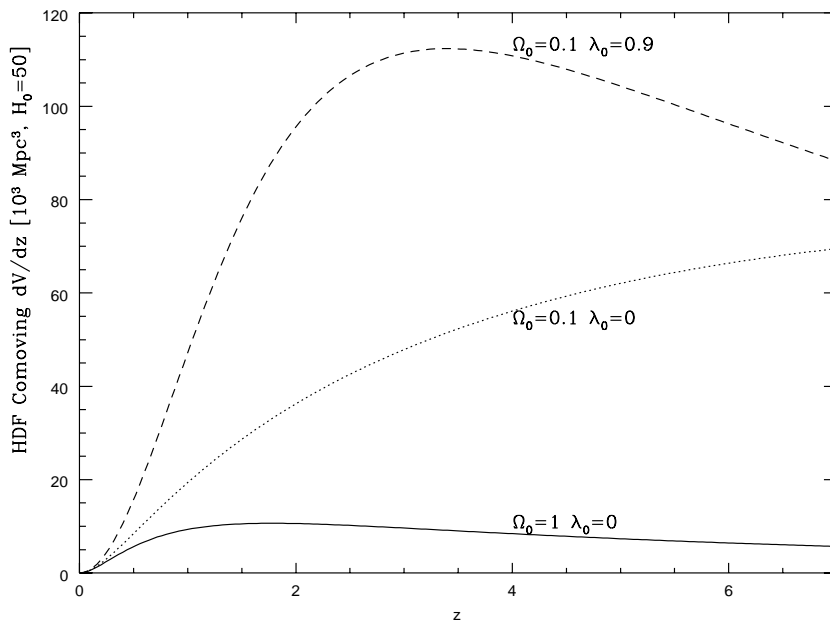


Figure 1: Differential comoving volume versus redshift in the Hubble Deep Field for three cosmological models. Note the order-of-magnitude difference between the models.

### 3 How to Observe High Redshift Galaxies?

The attempt to detect primeval galaxies by means of strong emission lines, particularly Ly $\alpha$ , has failed. Blind surveys for emission-line objects have covered more than  $10^6$  Mpc<sup>3</sup> with no detections.<sup>4</sup> We now understand that even a minuscule amount of dust can strongly attenuate the Ly $\alpha$  photons that are resonantly trapped in the emitting region.

High redshift galaxies are occasionally discovered serendipitously, for example when they are lensed by a foreground cluster.<sup>5</sup> More recently, a possible rich cluster of galaxies was identified at  $z = 2.56$  in a field in which there are two confirmed quasars of that redshift separated by 1'.5, and a nearby microwave background decrement that is plausibly explained as due to the Sunyaev-Zel'dovich effect.<sup>6</sup> The cluster candidates, which await spectroscopic confirmation, were identified by means of excess emission at the redshifted Ly $\alpha$  wavelength detected by medium-band imaging.

While such discoveries are of interest — even a single confirmed rich cluster at high redshift could significantly constrain some cosmological models — real understanding comes only with systematic surveys based on a successful detection scheme. Such a mechanism has become available only in the last few years, with the realization that absorption at the Lyman limit and in the Ly $\alpha$ -forest region lead to broad-band color features which provide reliable photometric redshift estimates.<sup>7</sup>

The need for photometric redshifts became acute as the limiting imaging magnitude was pushed to fainter limits than are accessible to spectroscopy, particularly the faint galaxies of the Hubble Deep Field (HDF). The methods for photometry and redshift estimates vary somewhat between different groups, but there is now agreement on the resultant redshifts, and they are in good agreement with spectroscopic redshifts where available.<sup>8</sup> In fact, the spectroscopy is not easy either, and under careful scrutiny more spectroscopic redshifts were found to be in error than photometric ones.<sup>9</sup>

### 4 What Have We Learned?

The first and foremost fact to emerge from the imaging of the HDF was the small angular size of the bulk of the galaxies. The right panel of Fig. 2 shows the angular distribution of all the HDF objects, most of which are  $\sim 0''.1$ . As the left panel of the figure shows, this corresponds to a size  $\lesssim 1$  kpc, and an inspection of the HDF images shows that most of them are blue. Hence, the excess faint blue galaxies are dwarfs, not large, high-redshift, elliptical galaxies.

Among the HDF galaxies are a handful of galaxies at photometric redshifts

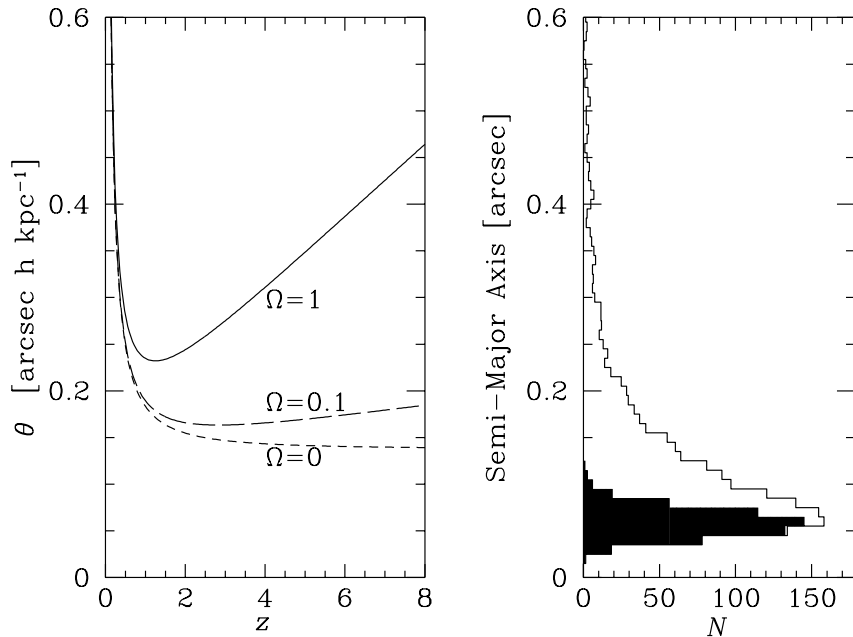


Figure 2: The expected relation between angular diameter and redshift for an object with proper size  $1h^{-1}$  kpc, compared with the actual distribution of diameters of galaxies in the Hubble Deep Field. The shaded part of the histogram are the counts of galaxies with magnitudes  $AB(8140) > 28$  where incompleteness sets it.

$z \gtrsim 5$ ,<sup>10,11</sup> the brightest of which are not much fainter than those observed spectroscopically. Fig. 3 shows an example of the spectral energy distribution of such a galaxy with no detection shortward of the F814W band, clear detection in the F814W and K bands and a probable one in the H band. Notice the small sizes of the error bars of the HST observations, which are almost imperceptible on the scale plotted. They severely constrain the spectral energy distributions that can be fitted to the data. The lower limit on the F814W/F606W flux ratio can also not be due to dust (in extraordinarily large amounts) because the spectrum would rise much more steeply into the IR, exceeding the observations. Finally, multiple-wavelength detection rules out the possibility of an emission-line galaxy, and the angular extension precludes a star. The only plausible explanation of the sharp drop in flux between the F814W and F606W bands is Lyman-limit and Ly $\alpha$ -forest absorption, placing the galaxy at redshift  $z \gtrsim 5$ .

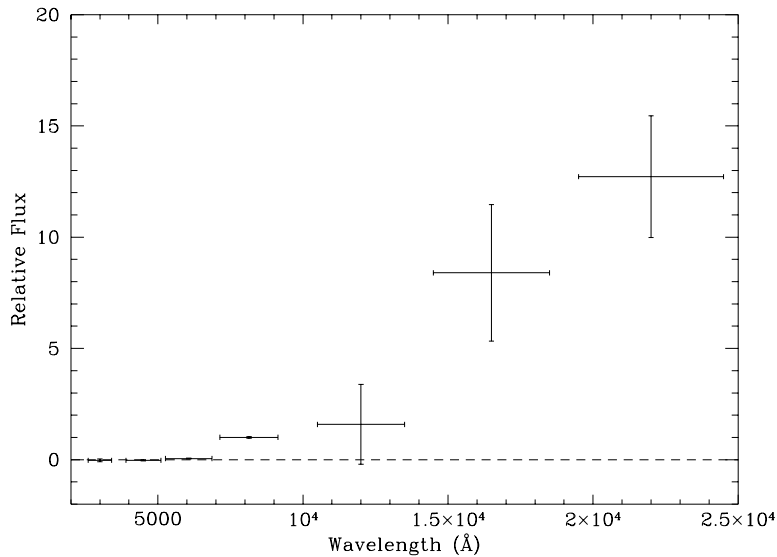


Figure 3: Spectral energy distribution of a galaxy with photometric redshift  $z > 5$ . Note the small sizes of the error bars of the HST observations, which are almost imperceptible on the scale plotted but severely constrain the spectral energy distributions that can be fitted to the data. The redshift estimate is based on the sharp drop in flux between  $6000\text{\AA}$  and  $8000\text{\AA}$ , which is attributed to Lyman-limit and  $\text{Ly}\alpha$ -forest absorption. Absorption by dust is ruled out because it would imply higher infrared flux than is observed.

The search for high-redshift galaxies can be extended further by looking for galaxies which show IR emission but no detection in any of the HST bands, including the F814W band. Fig. 4 shows the spectral energy distributions of five objects detected in the K band but not in the F814W band. If the drop in flux in the F814W band is due to Lyman-limit and  $\text{Ly}\alpha$  absorption, then the redshifts of these objects are in the range  $z = 7 - 17$ ; a more accurate determination awaits better photometry, particularly in the J and H bands.

Although it is very exciting to detect galaxies at higher redshifts than previously known, the most important ingredient to our understanding of galaxy formation and evolution comes not from those exceptional tails of the distribution but from the overall redshift distribution. Fig. 5 shows the photometric redshift distribution, whose most remarkable feature is the drop in counts at

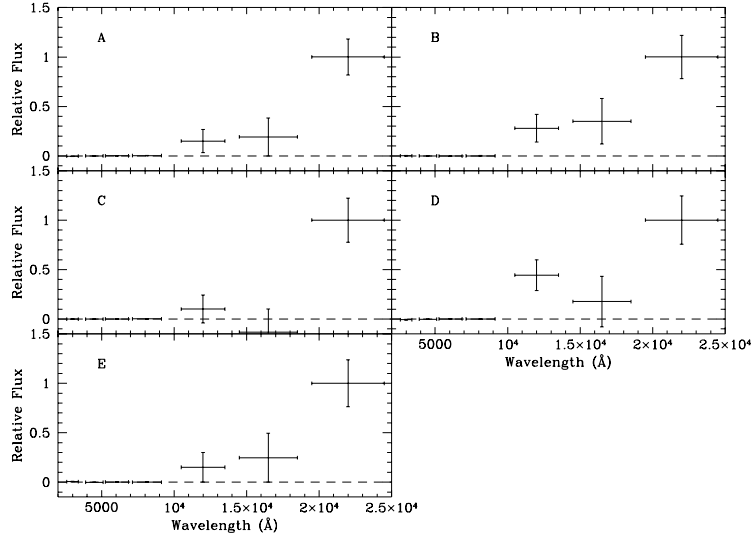


Figure 4: Spectral energy distributions of five objects detected in ground-based  $K$ -band imaging but not in the HST F814W band. Interpreting the drop in flux in the HST bands to be due to Lyman-limit and Ly $\alpha$  absorption, these objects have redshifts in the range  $z = 7 - 17$ .

redshifts  $z \gtrsim 2.5$ . A morphological breakdown of the redshift distribution shows, in fact, that spiral galaxies disappear quickly beyond  $z = 1$ , and elliptical galaxies beyond  $z = 2.5$ .<sup>12</sup> All the objects at higher redshifts are small, with sizes  $\sim 1$  kpc.

Recall that high-redshift galaxies are observed at rest-UV wavelengths, and that the UV emission in nearby galaxies is also confined to starbursting regions of comparable size.<sup>13</sup> It is therefore tempting to explain the small sizes of high-redshift galaxies as due to UV-producing starbursts in small regions of galaxies and not over an entire 10 kpc range.

However, the drop in the number counts of 10 kpc spirals at redshift  $z \approx 1$ , and that of the ellipticals at redshift  $z \approx 2.5$ , is quite sharp. The HDF is deep enough so galaxies with luminosities well below  $L_*$  can be detected. It can also be shown that the cosmological diminution of surface brightness, together

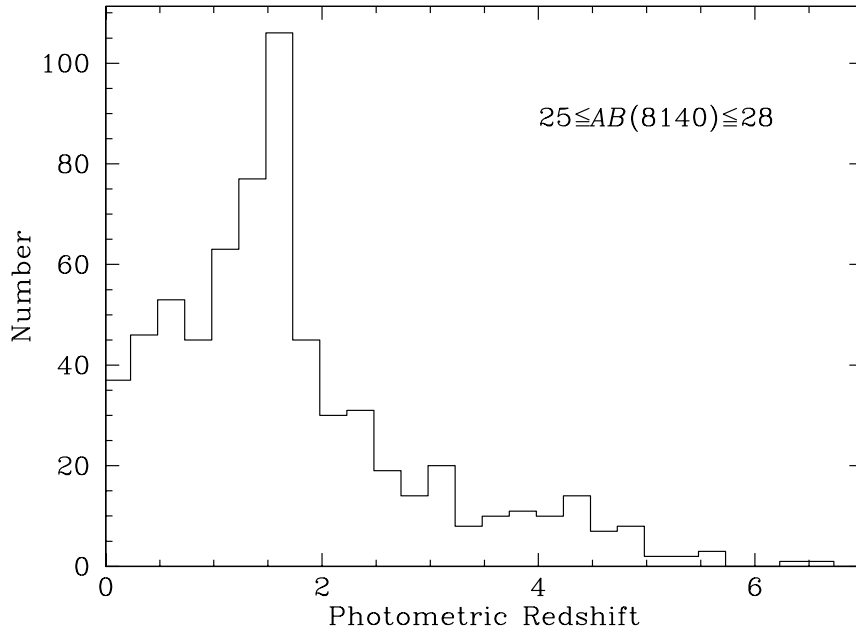


Figure 5: Distribution of photometric redshifts of all objects with magnitudes  $25 \leq AB(8140) \leq 28$  in the Hubble Deep Field. Note the decline in numbers for redshifts  $z \gtrsim 2.5$  and contrast it with the expected increase for constant comoving density, Fig. 1.

with the K-correction, are not the limiting factors for redshifts  $z \lesssim 2$  (spirals) and  $z \lesssim 4$  (ellipticals). Present day galaxies, evolved according to standard models,<sup>14</sup> would be observed to have larger sizes than the objects in the HDF. However, uncertainties in the evolutionary models, plus the unknown dust content of primeval galaxies, make it difficult to reach a firm conclusion.

It is clear that the redshift cutoff cannot be explained by having star formation take place entirely at lower redshifts, since this would violate observational limits from number counts and redshift surveys. If the galaxies were indeed small at high-redshift, they have had to grow by mergers (ellipticals), or star formation in their disks has had to proceed from the inside out (spirals).

Whatever the mechanism by which galaxies “hide” at high redshift, it is increasingly more difficult to conceal them in large-volume universes, such as open or  $\lambda$  universes with a low deceleration, Fig. 1. For those cosmological models the total number of observed galaxies is less than predicted, irrespective

of size. Star formation would then have to be episodal to account for the observed number of objects, and more of the star formation would have to take place behind a shroud of dust. Any realistic model of galaxy formation will have to face this issue, particularly if other observational evidence continues to point toward open or  $\lambda$  models, as it now increasingly does.

Further comments are given in the concluding remarks to this conference.

## 5 Where Do We Go From Here?

Based on the experience of the last few years we expect most progress to come from observations. Deep near-infrared imaging is very useful to improve the photometric redshifts of all fainter galaxies, and is essential for galaxies at redshifts  $z \gtrsim 5$ . Spectroscopy of Balmer lines can determine the dust content of the galaxies, telling us how much star formation is hidden from UV view. It will also confirm spectroscopic redshifts in the range  $1 < z < 2$ , which have not been adequately observed from the ground. Deep HST imaging in intermediate bands, especially at  $7000\text{\AA}$ , can improve the photometric redshifts and increase their reliability at fainter magnitudes. Finally, better image reconstruction should improve both resolution and photometry, enabling more accurate flux measurement and the detection of fainter objects.

On the theoretical side, modeling of galaxy formation is only beginning seriously to tackle gas dynamics and star formation. Expect important breakthroughs here.

In any event, we can no longer content ourselves with the traditional number counts,  $N(m)$ ,  $N(z)$ , or even  $N(m, z)$ . The sizes of galaxies at different wavelengths, or better yet their profiles, are observable and provide crucial constraints both to galaxy formation and to the underlying cosmological model. We need to obtain these data and to confront our models with them.

## Acknowledgments

This work was supported in part by NASA grant AR-07551.01-96A.

## References

1. B. M. Tinsley ApJ **241**, 41 (1980).
2. P. Madau, H. C. Ferguson, M. E. Dickinson, M. Giavalisco, C. C. Steidel, and A. Fruchter, MNRAS **283**, 1388 (1996).
3. For example, C. M. Baugh, S. Cole, C. S. Frenk, and C. G. Lacey, ApJ, in press (1998); preprint astro-ph/9703111.



4. D. Thompson and S. G. Djorgovski, *AJ* **110**, 982 (1995).
5. B. Frye and T. Broadhurst, *ApJ*, submitted, and references therein; preprint astro-ph/9712111.
6. A. Campos, A. Yahil, R. A. Windhorst, E. A. Richards, and S. Pascarella, *ApJ*, submitted (1998).
7. C. C. Steidel and D. Hamilton, *AJ* **104**, 941 (1992).
8. D. W. Hogg, et al., *AJ*, in press (1998); preprint astro-ph/9801133.
9. K. M. Lanzetta, A. Fernández-Soto, and A. Yahil, in *The Hubble Deep Field*, eds. M. Livio, S. M. Fall and P. Madau, in press; preprint astro-ph/9709166.
10. K. M. Lanzetta, A. Yahil, and A. Fernández-Soto, *Nature* **381**, 759 (1996).
11. K. M. Lanzetta, A. Fernández-Soto, and A. Yahil, *AJ*, submitted (1998)
12. S. P. Driver, A. Fernández-Soto, W. J. Couch, S. C. Odewahn, R. A. Windhorst, S. Phillipps, K. Lanzetta, and A. Yahil, *ApJ*, in press; preprint astro-ph/9802092.
13. G. R. Meurer, T. M. Heckman, C. Leitherer, A. Kinney, C. Robert, and D. R. Garnett, *AJ* **110**, 2665 (1995).
14. G. Bruzual and S. Charlot, *ApJ* **405**, 538 (1993); and later releases of computer codes.